Advances in Science and Technology Research Journal

Advances in Science and Technology Research Journal 2024, 18(1), 26–35
https://doi.org/10.12913/22998624/175676
ISSN 2299-8624, License CC-BY 4.0

Received: 2023.10.11
Accepted: 2023.12.22
Published: 2024.01.15

Evaluation of Structural Powder Steel Properties after High-Temperature Thermomechanical Treatment and Finish Turning

Kamil Leksycki[1*], Eugene Feldshtein[1], Radosław Maruda[1], Larisa Dyachkova[2], Natalia Szczotkarz[1], Alexandra Zverko[2]

[1] Faculty of Mechanical Engineering, University of Zielona Gora, 4 Prof. Z. Szafrana Str., 65-516 Zielona Góra, Poland

[2] The State Scientific Institution „Powder Metallurgy Institute", Belarusian National Academy of Sciences, 41, Platonov Str., 220005 Minsk, Belarus

* Corresponding author's e-mail: k.leksycki@iim.uz.zgora.pl

ABSTRACT

High-temperature thermo-mechanical processing (HTTMP) is a combination of plastic deformation and heat treatment operations. Such action makes it possible to increase metal mechanical properties resulting from both mechanical strengthening and heat treatment. As a result, it is possible to achieve high complex of operating characteristics of different types of steel and other alloys. However, there is a lack of information on the applicability of HTTMP of powder steel. These types of steel are very effective substitutes for traditional structural steel but are characterized by poor mechanical properties. This study considers the possibility of using HTTMP for powder steel frame additionally infiltrated by bronze with MoS_2 addition to increase mechanical properties of the materials studied. Steel infiltrated, infiltrated and then hardened, infiltrated and then HTTMP treated with strain rates of 30, 50 and 70% were compared. The microstructural properties and hardness of the materials before machining were studied as well as the cutting forces and surface topography of those materials after turning with AH8015 carbide inserts. Cutting forces tests were realized with v_c = 157 m/min, f = 0.25 mm/rev and a_p = 0.25 mm. Surface topography tests were carried out with v_c = 157 m/min, f = 0.25 mm/rev and a_p = 0.25 mm. Constant cutting parameters were used to eliminate the effects of rest factors. It was found that the lowest cutting forces (F_c, F_p and F_f), surface roughness parameters (*Sa* and *Sq*) and small areas with single high peaks on the machined surface were obtained for infiltrated powder steel with subsequent HTTMP machining under 50% strain rate.

Keywords: structural powder steel, infiltration, hardening, high-temperature thermo-mechanical processing, cutting force, surface texture.

INTRODUCTION

Modern machines are made of structural materials characterized by high mechanical and operational properties. Various methods of the material properties improving are known, such as heat and thermo-chemical treatment, traditional alloying and micro-alloying, surface treatment technologies, the use of multilayer materials, etc. For many years, this has also been achieved by high-temperature thermo-mechanical processing (HTTMP) of steel and other alloys. The HTTMP involves the steel hardening immediately after hot pressure exposure, when the metal has an austenitic structure. In the short time between the end of the deformation process and hardening, there is no time for recrystallization to occur. Therefore, the strengthening that occurred during the plastic deformation while rolling or forging is not eliminated and remains in the material after it has cooled down. After tempering, this is supplemented by strengthening due to the hard martensitic structure. The martensite formed under these conditions inherits, in addition to its

own dislocations, the dislocations that arose during the work stressing. It is clear that the shorter the time interval between the completion of all processes, when the steel is of high-temperature, the more dislocations are retained, and the greater the strengthening effect is shaped. Practically, this time interval is a few seconds during which recrystallization partially occurs and which reduces the strengthening effect. Recrystallization is one of the main drawbacks of the steel HTTMP.

Actually, HTTMP is an integral part of production of many types of steel, ranging from carbon steel to alloyed grades. Advanced low-carbon plate steel are now increasingly manufactured and their production process combines controlled hot rolling with accelerated cooling to regulate the microstructure through the processing. HTTMP has led to the development of new grades of steel with highly desired combinations of properties that would have been impossible to achieve with more conventional processing approaches. These steel products cover an extremely wide range of applications, including gas and fuel transportation pipes, high-rise buildings, car park decks, bridges, power transmission towers, lightning poles, building beams and panels, shipbuilding, car bodies, rail tracks, and transformer sheets, among others.

HTTMP technologies demonstrate their effectiveness for a wide range of steel and other alloys, such as conventional and advanced ones. However, there is a lack of information on the possibilities of materials made with powder metallurgy (PM) methods after HTTMP. PM materials are used in a wide range of applications, such as friction and antifriction, tooling, filtering, structural and other materials. Most of them have residual porosity, which significantly reduces strength and thermal conductivity and increases their brittleness. An effective way to prevent this phenomenon is infiltration with molten additive material, which fully eliminates the pores.

Although produced in near-net shapes, most components fabricated from PM materials still require some form of secondary machining. Nevertheless, there are not many studies on the machinability of these materials, despite the fact that machining accounts for more than 15% of the value of all products manufactured in industry [1]. Salak et al. [2] reported that the machinability of PM steel can be improved in a number of ways, such as by influencing the work-piece material properties in a targeted manner, adding various pore-closing additives by impregnation or infiltration, modifying the microstructure by alloying as well as using appropriate heat treatment processes and the right choice of tool material and cutting conditions. Possible combinations of these approaches offer many options for improving the machinability of PM steel. In terms of characterizing the material properties in relation to machinability, it is possible to define two groups of PM steel. The first group includes Fe-C steel, which can be characterized quite easily on the basis of hardness and the proportion of ferrite and perlite. The second group includes alloy steel, which are more complicated to characterize the properties of the work-piece in relation to the cutting process. Data on the machinability of PM steel can help evaluate the actual technical and economic efficiency of the machining methods used. Okimoto [3] described resin impregnating into the open pores of a sintered iron compacts and revealed the improvement of their machinability due to reduction in the plastic deformation during the chip formation, the decrease of the work hardening and the reduction of the cutting force. Tutunea-Fatan et al. [4] considered one of the fundamental parameters used to describe the cutting forces. Experiments conducted with porous titanium revealed a relative relationship between the magnitude of the cutting force and the porosity of this material. Shin and Dandekar [5] informed that metal matrix composites (MMCs) as advanced structural materials based on metal powders have a high strength-to-weight ratio, high stiffness and good damage resistance over a wide range of operating conditions. The authors considered the details of changes in the cutting forces, chip morphology, temperature and subsurface damage compared to conventional materials. Sadat [6] stated that the applications of traditional machining processes usually lead to the surface and subsurface changes that differ from the base materials. In order to avoid the unwanted changes that can negatively affect the work-piece quality, it is necessary to know the different types of machining transformations and their provenance. It is also important to know the cutting parameters and tool geometry that will lead to high-quality of work-piece. Ilio and Paoletti [7] determined that MMCs machining is difficult due to the presence of two or more separate phases, one of which is highly abrasive, and the distinct differences between the hard ceramic reinforcement and the ductile metal matrix. Parts made from MMCs must always be machined to conform to the final

design requirements. Pramanik and Zhang [8] studied the particle cracking and detachment during the machining of MMCs and revealed that it was due to the occurring stresses and strains and interactions with the cutting tool and with other particles. Obikawa et al. [9] analyzed Fe-2Cu-0.8C sintered steel cutting under different lubrication/cooling conditions and with different tool materials and revealed that thick coating of the carbide tool is effective for considerable improvement of the machinability of this steel. Kulkarni and Dabhade [10] studied machinability of Fe-Cu-C sintered alloys and revealed that MnS added in the alloys tested provided improving of the post-sinter machining performance. Li and Laghari [11] analyzed the conventional machining processes for MMCs and discussed the tool wear, MMCs machinability and surface quality for different manufacturing processes. Comprehensive problems and conclusions concerning the machining of particle-reinforced MMCs were elaborated. Ebersbach et al. [12] analyzed the effect of cutting parameters on force, texture and chip morphology under turning of self-lubricating carbon steel with addition of Ni, Si and h-BN particles. All the studied materials were manufactured under single pressing and double pressing. It was revealed that all components of the resulting cutting force were 10–25% higher after double pressing compared to single pressing. *Sz* texture parameters were lower for double pressing compared to single pressing. The segmented chip was observed and K_h value was affected by the cutting parameters and manufacturing features. Xu et al. [13] investigated the effect of machining parameters using monocrystalline diamond tools on the pore structures of sintered bronze. It was found that turning with diamond tools provided effective machining of porous bronze and solved the problem of pore blockage in the porous materials. Sap et al. [14] studied the machinability of Cu-composites with Ti-Be-SiC particle additives and a significant impact of speed and feed on the surface roughness, cutting wear and temperature as well as chip morphology was observed. Kulkarni et al. [15] tested machining "green/un" sintered powder steel. The authors found that the tested material increased brittleness, which caused damage to the cutting edge and worsened the roughness of the machined surface. This can be remedied by increasing the cutting speed and feed rate, but the results are worse compared to hardened (sintered) materials. As it was shown above, there are not many scientific papers in the current literature on the machinability of materials made by PM methods after HTTMP. On the other hand, HTTMP powder steels are materials that can replace conventional structural steels, but have poor mechanical properties. This study considers the possibility of using HTTMP for powder steel frame additionally infiltrated by bronze with MoS_2 addition to increase mechanical properties of the materials studied.

The aim of this study is to analyze the effect of high-temperature thermo-mechanical processing of carbon sintered steel on the microstructural properties and hardness as well as on the cutting forces and surface topography after finish turning process.

MATERIAL AND METHODS

The materials studied were manufactured by infiltration of CuSn5 tin bronze pressed into powdered steel frame. As frames, Fe-base green samples had 1.2% graphite addition and were produced according to the technology described by Dyachkova and Feldshtein [16]. The samples were pressed to form rolls of 50 mm in diameter and obtain relative density of 82–83%. Infiltrating material was produced by mixing in a ball mixer of a "drunken barrel" type for 1,5 h of powders of iron, pencil graphite, copper, tin and molybdenum disulfide. Additionally, 5% of iron and 1.5% of special compounds were added in the charge mixture in order to exclude erosion under infiltration. The infiltration of initial frames after pressing was carried out under an endothermic gas atmosphere at 1140 °C. Final material composition is presented in Table 1. The real density of in-situ steel frame was 80–81% and after infiltration, hardening and HTTMP, it was 96–98%.

Since the materials studied have an increased corrosion resistance, the heating of samples during hardening and HTTMP was performed in air. Hardening was performed at the temperature of 800 °C in water, after which, the samples were tempered at 200 °C during 1 h. HTTMP was performed as follows: heating at the temperature of 800 °C, deformation by stamping at 750 °C with the steps of 30% and 50%, rapid cooling (hardening) in water, tempering at 200 °C and 500 °C during 1 h. The structure was studied using a MEF-3 metallographic microscope as well as a Mira electron microscope with an INCA 350 apparatus of Oxford Instruments, designed for

Table 1. Final material composition, %

Gr	MoS_2	Cu	Sn	Fe
1.2	1	17	1	The rest

micro-X-ray spectral analysis. Microstructural sections of the materials were made in the direction parallel and perpendicular to the direction of pressure action and then the surfaces were etched with 4% solution of picric acid in ethanol.

Turning tests were carried out on a CNC CKE6136i DMTG lathe. The turning tool consisted of a SDJCR 20x20 K11 tool holder with a DCMT11T304-PSS cemented carbide insert of AH8015 grade of Tungaloy. Inserts were PVD coated and nano-multilayer TiAlN coating was used. The insert and its geometrical dimensions are shown in Figure 1. The cutting parameters of studied machinability features are shown in Table 2. A 9129AA piezoelectric multicomponent dynamometer by Kistler (Fig. 1 b) was used to register components of the cutting forces (F_c – cutting force, F_p – passive force, F_f – feed force) and the sampling rate was of 10000 Hz.

The dynamometer consists of piezoelectric measuring sensors, which were mounted under a high pre-voltage, between the upper plate and the base plate. Each sensor contains three pairs of quartz platelets. One pair is responsible for measuring force in the Z-axis direction, while the others are responsible for measuring forces in the X- and Y-axis directions. Processing, visualization, and recording of signals were carried out using Dyno Ware software. To measure the surface topography of the samples tested, a Sensofar S Neon Optical profiler was used. For statistical analysis of the test results, the tests were repeated 3 times.

RESULTS AND DISCUSSION

Microstructure changes

The study of samples after infiltration revealed that their micrstructure consists of areas of steel frame with perlite structure with a small amount of cementite and areas of copper phase, located on the borders and at the junctures of frame (Fig. 2). The microstructure of the steel frame is practically homogeneous in respect to carbon. Inclusions of sulfides are located in iron-based partials, but predominantly in the copper phase. Molybdenum disulfide decomposes during infiltration to form sulfide Mo_2S_3 and free sulfur, which forms copper sulfides, interacting with copper. Hardening of the samples led to the formation of a troostite-martensite microstructure (Fig. 3). During heating, the diffusion of copper from the grain borders of

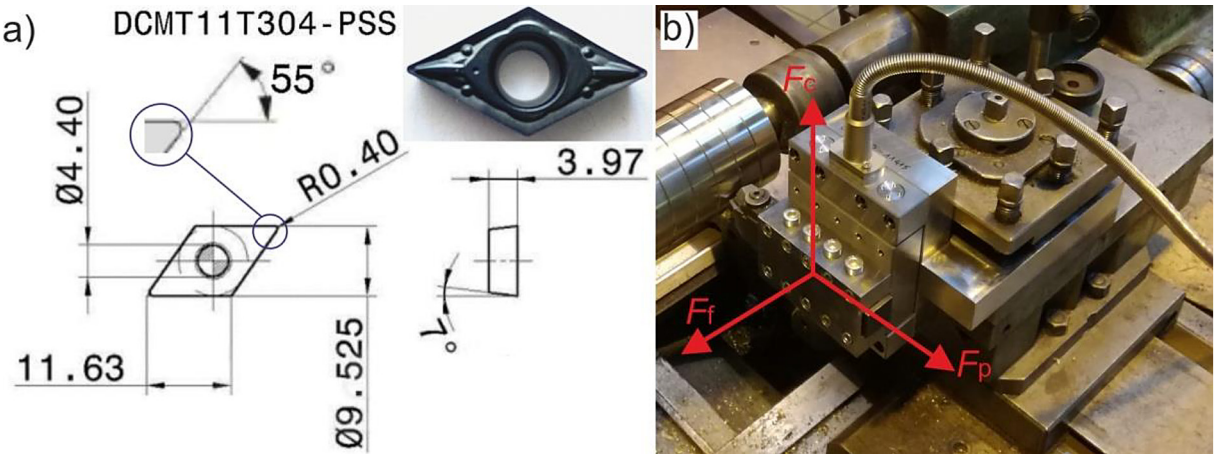

Figure 1. The insert and its geometrical dimensions (a) and a scheme of cutting forces action in the Kistler dynamometer (b)

Table 2. Cutting parameters of the studied machinability features

Machinability features	Cutting speed (v_c), m/min	Feed rate (f), mm/rev	Depth of cut (a_p), mm
Cutting forces	157	0.05	0.25
Surface texture	50	0.15	

the steel frame to its center occurs, carbon content at the borders with the copper phase increases and a 2–5 μm thick layer is formed there.

The study of the tested material microstructure processed using HTTMP showed that under deformation, a macro-texture is formed and the microstructure in the direction parallel and perpendicular to the pressure direction is different (Fig. 4). After HTTMP with the strain rate of 30% in the direction parallel to the pressure action and tempering at 200 °C, a decrease in the grain size in the steel frame and the appearance of more thin zones of the copper phase (Fig. 4 a) was observed. Smaller grains in the steel frame have the microstructure of unstructured martensite and troostite-martensite, whereas larger grains have troostite microstructure with residual finely dispersed austenite inclusions (Fig. 4 b). Under tempering at 500 °C, residual austenite decomposes, the microstructure of the steel frame becomes mainly bainite and the copper phase is subjected to aging, as evidenced by the ultra-dispersed phases observed.

Increasing the strain rate up to 50 % leads to even greater fragmentation of the steel frame structure, a decrease in the thickness of the copper phase interlayers (Fig. 5) and also an increase in the residual austenite content up to 20–25%. The copper amount and carbon homogeneity in the steel areas increase due to the increased number of defects and the acceleration of the diffusion processes. The structure of the steel frame is structureless martensite.

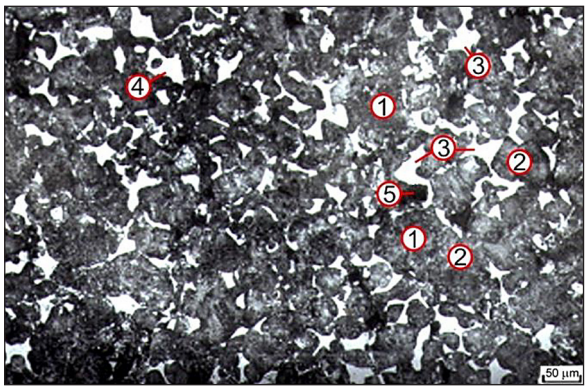

Figure 2. Microstructure of the material tested after infiltration: 1 – sections of steel frame with perlite structure; 2 – cementite inclusions; 3 – areas of copper phase; 4 – sulfide inclusions in copper phase; 5 – sulfide inclusion in the steel frame

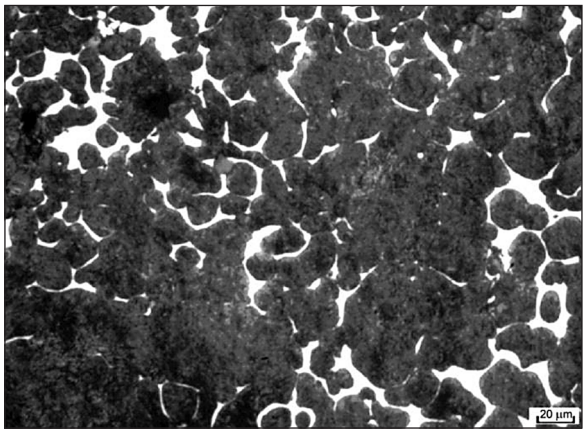

Figure 3. Microstructure of the material tested after hardening and low tempering

Hardness changes

HB hardness of the materials tested depends on the processing technologies (Fig. 6). It can be seen that the results varies quite a bit. This is due to the simultaneous interaction of various mechanical loads and high temperatures as a result of which microstructural and phase changes occur and new compounds are formed. Such changes provides to relatively stable deviation (not exceeding 5%). Porous steel frame has the lowest HB, infiltration as well as infiltration followed by hardening increases HB by about five times, with the residual porosity reducing to 2–4%. HTTMP with 30% strain rate and followed by tempering increases hardness up to 20%. Further increase of the strain rate up to 50% leads to the following HB growth of about 5%, however, the strain rate increases up to 70% providing 5% HB decrease. As mentioned above, the recrystallization that leads to a reduction in strengthening, occurred during HTTMP. Because of this phenomenon, it is recommended that the strain rate when using HTTMP for functional materials does not exceed 20–30%. In the authors' opinion, the presence of ductile bronze areas due to infiltration of the in-situ powder steel increases the allowable strain rate of PM of steel from 30 up to 50%.

Cutting forces changes under turning process

As an example, the time course of changes in the cutting forces when turning the material after infiltration are shown in Figure 7. The noticeable cyclic changes are due to the presence of a thin component (bronze) in the work-piece material. Such changes can cause an intermittent peeling of the surface machined.When analyzing the impact

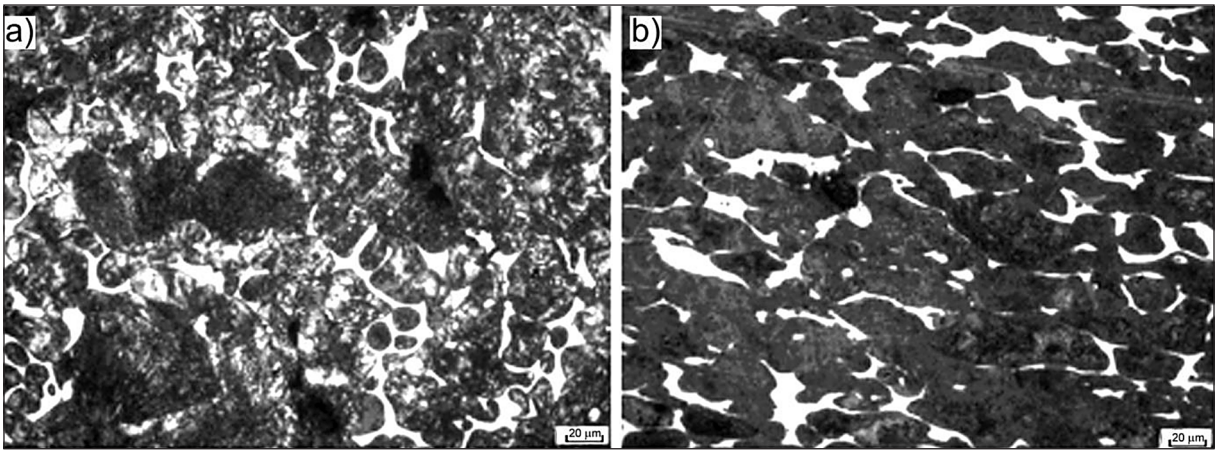

Figure 4. Microstructure of the material tested after HTTMP with 30 % strain rate and tempering at 200 °C: (a) in the direction parallel to the pressure action; (b) in the direction perpendicular to the pressure application

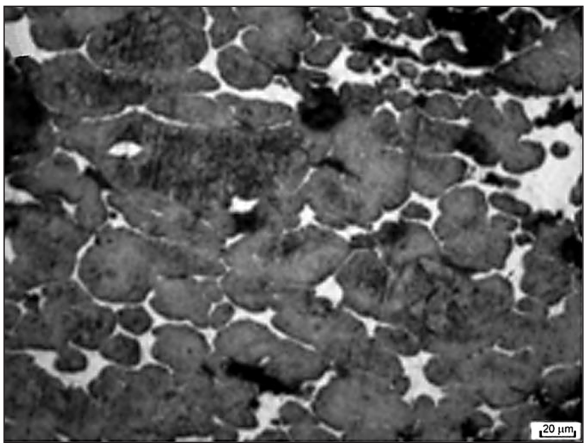

Figure 5. Microstructure of the material tested after HTTMP with 50 % strain rate and tempering at 550 °C

of the tested materials manufacturing technology on the average cutting forces changes (Fig. 8), it was observed that the force changes are similar to changes in the hardness of these materials, which is a typical correlation in case of structural materials turning [17]. Relatively large variations in the average force values can be justified by the presence of a thin component in materials. Depending on the material tested, the changes in F_c force are of 7–23%, F_p of 5–59% and F_f of 13–69%. Such significant changes are caused by the simultaneous effect of the mechanical and structural properties of the materials tested as well as the cross-section of the uncut layer on the cutting force.

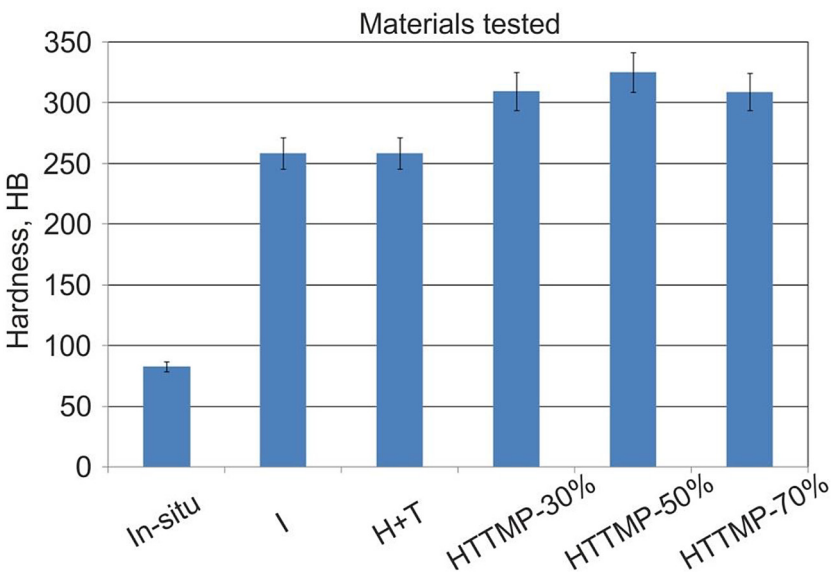

Figure 6. Hardness changes depending on the materials studied (I – after infiltration, H+T – after hardening and low tempering, HTTMP – as above)

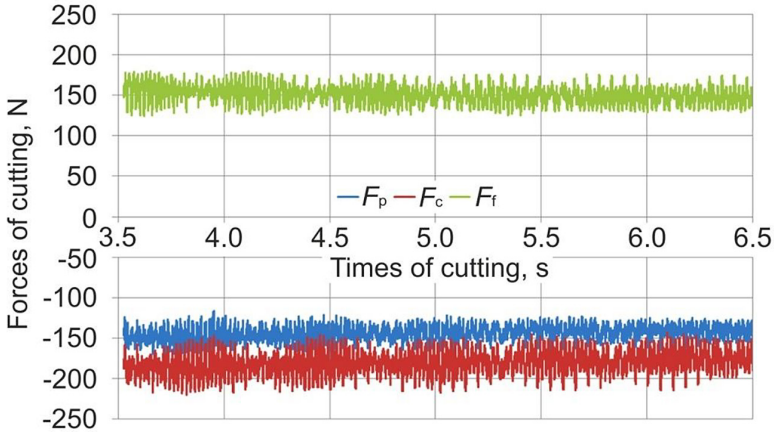

Figure 7. Changes in the cutting forces depending on the time of cutting when turning the material after infiltration

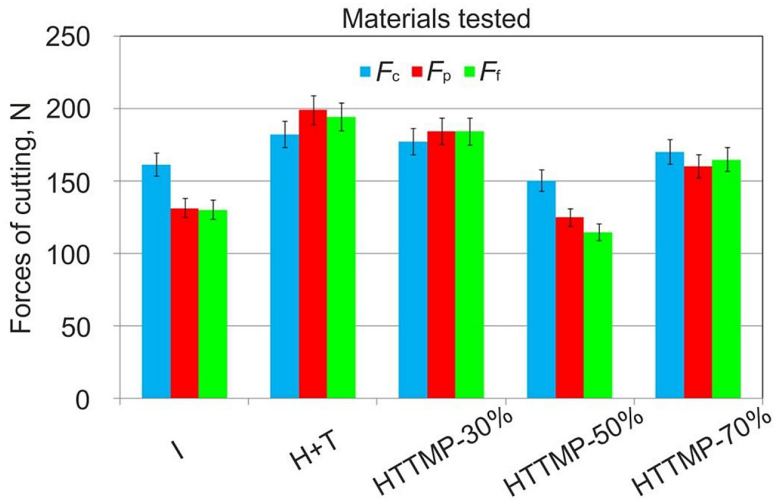

Figure 8. Average cutting forces changes depending on the materials studied (I – after infiltration, H+T – after hardening and low tempering, HTTMP – above)

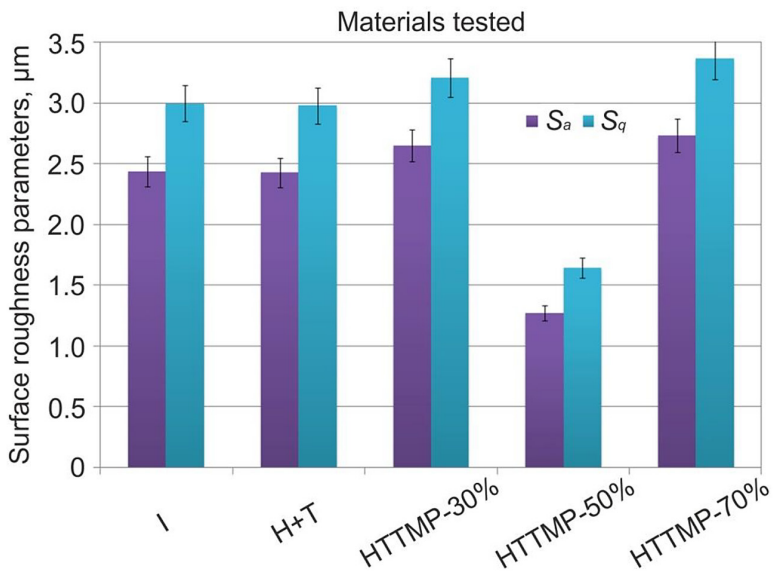

Figure 9. *Sa* and *Sq* parameters depending on the materials studied (I – after infiltration, H+T – after hardening and low tempering, HTTMP – above)

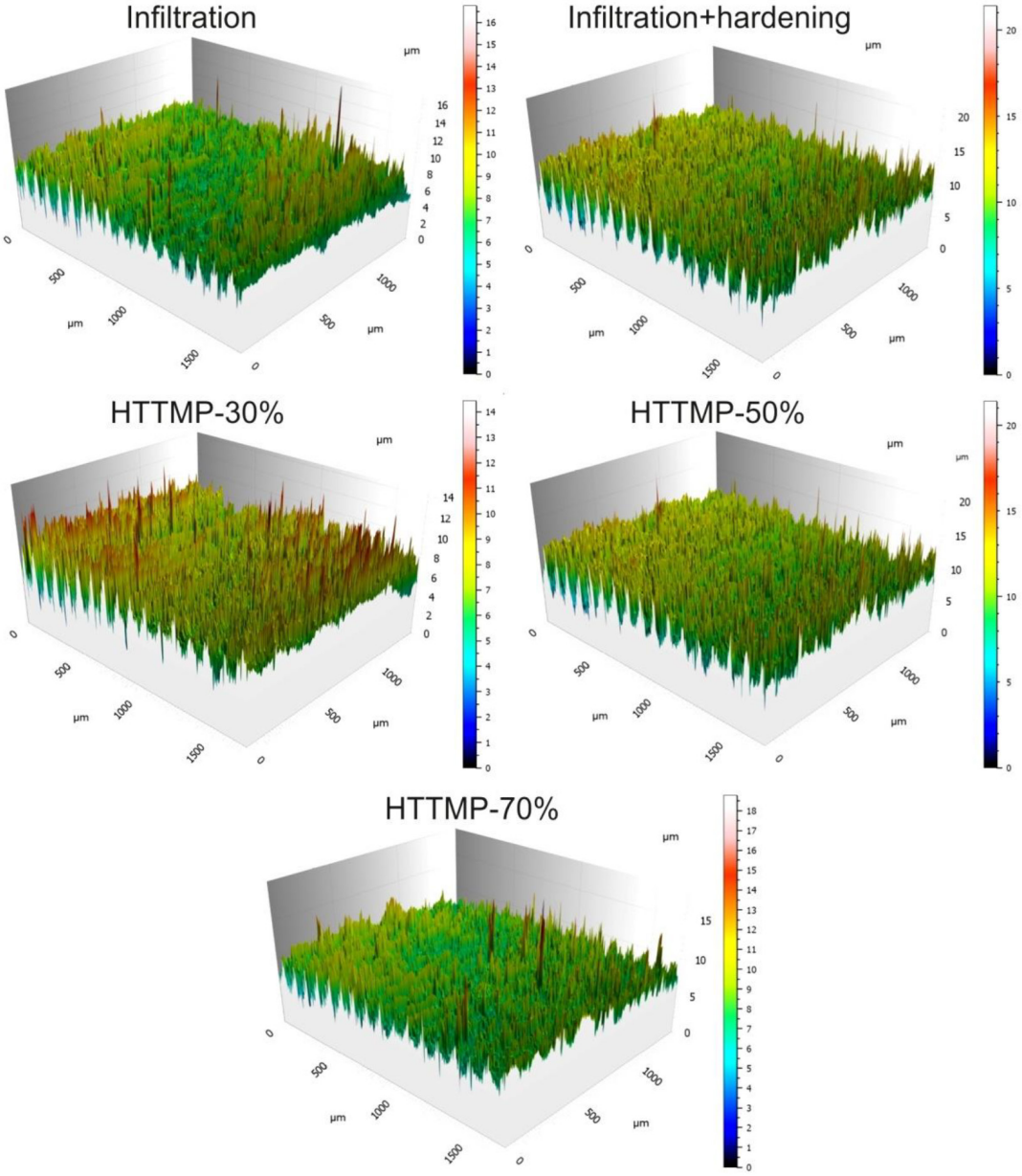

Figure 10. Three-dimensional images of the surface after strengthening and followed by turning

Surface texture changes after turning process

The changes in the *Sa* and *Sq* parameters of the surface texture of the tested materials are shown in Figure 9. These changes depend on conditions of the material strengthening, and the smallest of them are registered under HTTMP of 50%. Depending on the material tested, the changes in *Sa* and *Sq* parameters are of 91–115% and of 82–105%, respectively. Similar changes were observed in three-dimensional images of the surface after turning (Fig. 10). The most uniform topography with the small areas with single high peaks is characteristic of materials under 50% strengthening. In comparison, significantly more surface defects are observed on the surfaces after finish turning of iron-based MMCs reinforced with graphite and hard nano-oxides [18]. Similar particularities were observed by Feldshtein et al. [19].

CONCLUSIONS

In this paper, the microstructure and hardness of the structural powder steel after high-temperature thermo-mechanical processing were specified as well as the cutting forces and surface topography after finish turning. The following relationships were found. Microstructure of the materials tested consists

of areas of the steel frame with perlite structure with a small amount of cementite and areas of the copper phase located on the borders and at the juncture of the steel frame. The structure of the steel frame is practically homogeneous. Hardening leads to the formation of a troostite-martensite structure. During heating, the carbon content at borders with the copper phase increases and a 2–5 μm thick layer is formed there. After HTTMP with the strain rate of 30% in the direction parallel to the pressure action and tempering at 200 °C, a decrease in the grain size in the steel frame was observed. Smaller grains in the steel frame have the structure of unstructured martensite and troostite-martensite, whereas, larger grains have troostite structure with residual finely dispersed austenite inclusions. Increasing the strain rate up to 50 % leads to even greater fragmentation of the steel frame structure, a decrease in the thickness of copper phase interlayers. HB hardness of the materials tested depends on the processing technologies. Porous steel frame has the lowest HB, an infiltration as well as an infiltration followed by hardening increases HB by about five times. The HTTMP with 30% strain rate and tempering afterwards increases hardness up to 20%. Further strain rate increased up to 50%, leads to the following HB growth of about 5%, however strain rate increased up to 70%, provided 5% HB decreasing. As mentioned above, the recrystallization that leads to a reduction in strengthening, occurred during HTTMP. It is recommended that the strain rate for HTTMP PM of steel should be 30–50%. Some noticeable cyclic changes are observed due to the presence of a thin bronze in the materials tested. Dependency of changes in the hardness and cutting forces (F_c, F_p, F_f) of the materials tested was observed. Depending on the material tested, the changes in F_c force are up to 23%, F_p up to 59% and F_f up to 69%. Changes in the *Sa* and *Sq* surface texture parameters depend on conditions of the material strengthening, and the smallest of them are registered under HTTMP of 50%. Depending on the material tested, the changes in *Sa* and *Sq* parameters are up to 115% and 105%, respectively. The most uniform topography with the small areas with single high peaks is characteristic of the materials under 50% strengthening.

Acknowledgment

The authors would like to thank "Tungaloy Polska Sp. z o.o." for donating the cutting tools and making the research and preparation of this scientific paper possible.

Funding

This research was funded by the Polish Minister of Education and Science under the program "Regional Initiative of Excellence" in 2019–2023, project No. 003/RID/2018/19, funding amount PLN 11 936 596.10.

REFERENCES

1. Leksycki K., Maruda R.W., Feldshtein E., Wojciechowski S., Habrat W., Gupta M.K., Królczyk G.M. Evaluation of tribological interactions and machinability of Ti6Al4V alloy during finish turning under different cooling conditions. Tribology International 2023; 189: 109002.
2. Salak A., Selecka M., Danninger H. Machinability of powder metallurgy steels. Cambridge International Science Publishing, Cambridge, UK, 2005.
3. Okimoto K. Cutting mechanism of resin impregnated sintered iron. Materials Science Forum 2010; 638–642: 1836–1841.
4. Tutunea-Fatan O.R., Fakhri M.A., Bordatchev E.V. Porosity and cutting forces: from macroscale to microscale machining correlations. Proceedings of the Institution of Mechanical Engineers, Part B: Journal of Engineering Manufacture 2011; 225(5): 619–630.
5. Shin Y.C., Dandekar C. Mechanics and modeling of chip formation in machining of MMC. In: Machining of Metal Matrix Composites, J.P.Davim (red.). Springer, London 2012, 1–49.
6. Sadat A.B. Surface integrity when machining metal matrix composites. In: Machining of Metal Matrix Composites, J.P.Davim (red.). Springer, London 2012, 51–62.
7. Ilio A.D., Paoletti A. Machinability aspects of metal matrix composites. In: Machining of Metal Matrix Composites, J.P.Davim (red.). Springer, London 2012, 63–77.
8. Pramanik A., Zhang L.C. Particle fracture and debonding during orthogonal machining of metal matrix composites. Advances in Manufacturing.2017; 5: 77–82.
9. Obikawa T., Ohno T., Maetani T., Ozaki Y. Machining of sintered steel under different lubrication conditions. Machining Science and Technology, An International Journal 2018; 22(2): 338–352.
10. Kulkarni H., Dabhade V.V. Influence of MnS in Processing and Applications of Sintered Fe-Cu-C Alloys: An Overview. Materials Today: Proceedings 2018; 5(9): 17277–17283.
11. Li J., Laghari R.A. A review on machining and optimization of particle-reinforced metal matrix composites, The International Journal of Advanced Manufacturing Technology 2019; 100: 2929–2943.

12. Ebersbach F.G., Builes S.D., Dorneles C.F., Schroeter R.B., Binder C., Klein A.N., Biasoli de Mello J.D. Effect of cutting parameters in machining force, surface texture and chips morphology obtained in turning of sintered self-lubricating composites. Materials Research 2020; 23(4): 0120.
13. Xu J., Zhang X., Zhu F. Effects of machining parameters on surface morphology of porous bronze during monocrystalline diamond cutting. International Journal of Mechanical Sciences 2022; 234: 107686.
14. Sap S., Uzun M., Usca U.A., Pimenov D.Y., Giasin K., Wojciechowski S. Investigation of machinability of Ti-B-SiCp reinforced Cu hybrid composites in dry turning. Journal of Material Research and Technology 2022; 18: 1474-1487.
15. Kulkarni H., Dabhade V.V., Blais C. Analysis of machining green compacts of a sinter-hardenable powder metallurgy steel: A perspective of material removal mechanism. CIRP Journal of Manufacturing Science and Technology 2023; 41: 430–445.
16. Dyachkova L.N., Feldshtein E.E. Microstructures, strength characteristics and wear behavior of the Fe-based P/M composites after sintering or infiltration with Cu–Sn alloy. Journal of Materials Science & Technology 2015; 31: 1226–1231.
17. Klocke F. Manufacturing Processes 1. Cutting. Springer-Verlag, Berlin, Heidelberg, 2011.
18. Maruda R., Leksycki K., Feldshtein E., Sąsiadek E., Szczotkarz N., Odważna M., Ochał K., Gradzik A. Effects of hard oxides reinforcing of iron-based mmcs on the surface topography features after finish turning. Advances in Science and Technology Research Journal 2023; 17(1): 15–22.
19. Feldshtein E., Józwik J., Legutko S. The influence of the conditions of emulsion mist formation on the surface roughness of AISI 1045 steel after finish turning, Advances in Science and Technology Research Journal, 2016; 10(30): 144–149.